
MODELING EPIDEMIOLOGICAL DYNAMICS UNDER ADVERSARIAL DATA AND USER DECEPTION

Yiqi Su
Virginia Tech
Alexandria, VA 22305
yiqisu@vt.edu

Christo Kurisumoottil Thomas
Worcester Polytechnic Institute
Worcester, MA 01609
cthomas2@wpi.edu

Walid Saad
Virginia Tech
Alexandria, VA 22305
walids@vt.edu

Bud Mishra
New York University
New York, NY 10012
bud.mishra@gmail.com

Naren Ramakrishnan
Virginia Tech
Alexandria, VA 22305
naren@vt.edu

ABSTRACT

Epidemiological models increasingly rely on self-reported behavioral data such as vaccination status, mask usage, and social distancing adherence to forecast disease transmission and assess the impact of non-pharmaceutical interventions (NPIs). While such data provide valuable real-time insights, they are often subject to strategic misreporting, driven by individual incentives to avoid penalties, access benefits, or express distrust in public health authorities. To account for such human behavior, in this paper, we introduce a game-theoretic framework that models the interaction between the population and a public health authority as a signaling game. Individuals (senders) choose how to report their behaviors, while the public health authority (receiver) updates their epidemiological model(s) based on potentially distorted signals. Focusing on deception around masking and vaccination, we characterize analytically game equilibrium outcomes and evaluate the degree to which deception can be tolerated while maintaining epidemic control through policy interventions. Our results show that separating equilibria—with minimal deception—drive infections to near zero over time. Remarkably, even under pervasive dishonesty in pooling equilibria, well-designed sender and receiver strategies can still maintain effective epidemic control. This work advances the understanding of adversarial data in epidemiology and offers tools for designing more robust public health models in the presence of strategic user behavior.

Keywords Epidemiological modeling · Signaling games · Equilibrium analysis

1 Introduction

Epidemiological modeling increasingly depends on large-scale, crowdsourced behavioral data to track and forecast disease transmission dynamics in real time [3, 5]. Beyond clinical surveillance and mobility records, self-reported behavioral information on individual vaccination compliance, mask usage, and adherence to social distancing has become central to capturing the effects of non-pharmaceutical interventions (NPIs) [6].

However, empirical studies across diverse contexts demonstrate large and persistent gaps between self-reported and directly observed behaviors. For example, a national study in Kenya found that while only 12% of individuals reported not wearing masks, direct observation revealed that nearly 90% were non-compliant, a discrepancy exceeding 75 percentage points that was consistent across demographic groups [19]. Similar survey-based studies in countries like the USA document substantial social-desirability and recall biases in self-reported masking and vaccination behavior, compounded by spatial heterogeneity, policy variation, and limited auditability of daily behaviors [34]. While vaccination records are more structured and exhibit higher fidelity than other NPI measures, they nevertheless

exhibit persistent misreporting rates of approximately 5–15%, driven by reporting delays, incomplete registries, and misclassification errors [16, 10, 18].

Moreover, a persistent and underexamined challenge lies in the strategic nature of self-reported data. Individuals may misreport or withhold behavioral information to avoid penalties, retain access to workplaces or social benefits, or due to distrust in public health authorities (PHA) [22, 31]. In such settings, reported data can no longer be treated as passively sampled observations, but instead constitute strategic signals. This misalignment between reported and actual behavior can introduce systematic underestimation of key parameters and impair NPI effectiveness, as demonstrated by recent studies [39, 28, 25]. Unfortunately, state-of-the-art models largely fail to account for strategic misreporting by the population [27] and the few studies that do acknowledge parameter uncertainty (e.g., [33]) view it solely as an estimation problem rather than as a dynamic behavioral process that can be explicitly modeled.

To address these issues, we propose a game-theoretic framework that explicitly models the interaction between individuals and a cognizant public health authority (hereinafter, referred to as PHA) as a *signaling game* [32]. In our formulation, each individual (sender) chooses whether and how to report their health behavior (e.g., vaccination, masking), while the PHA (receiver) interprets these signals to estimate key epidemiological parameters and adjusts its recommendations accordingly. Crucially, both players act under bounded rationality and operate with partial information, yielding a dynamic interplay between strategic communication and epidemic control. This approach integrates rational speech act (RSA) models [12], which formalize communication as recursive reasoning between senders and receivers with epidemiological compartmental dynamics, offering a principled way to integrate behavioral information into epidemic forecasting. Our key contributions are:

- **Game-theoretic epidemic model.** We couple a stochastic compartmental model with a two-player signaling game, allowing the PHA to infer credibility and account for strategic misreporting rather than assuming truthful reporting, and to design policies that remain effective even when behavioral observations are adversarial.
- **Equilibria characterization and policy design.** By characterizing the signaling-game equilibria, we identify when truthful reporting can arise and how policy levers can be tuned to deter strategic misreporting while preserving predictive fidelity. Building on these insights, we design an adaptive feedback policy that weights reported data by inferred credibility to maintain the controlled reproduction number $R_c \leq 1$.
- **Generalizable simulation pipeline.** Rather than focusing on epidemic forecasting, we develop a generalizable modeling and simulation framework that integrates signaling-game equilibria with epidemiological dynamics to study how behavioral deception interacts with policy adaptation and epidemic control. The framework enables systematic evaluation of intervention strategies under varying behavioral and epidemiological assumptions, advancing the study of adversarial data in epidemiology and supporting robust public-health decision-making in the presence of strategic user behavior.

2 Related Work

Compartmental epidemiological models. Classical models such as SEIR have been extended with compartments for vaccination (V) and asymptomatic transmission (A), yielding SVEAIR models effective at reproducing COVID-19 dynamics [8]. Recent advances embed epidemiological models in neural ODE/SDE frameworks with transmission graphs and uncertainty-aware control [35, 38, 21]. Our approach builds on this line of research, adding process noise, weekly time-steps, and explicit feedback from reported behavior to policy, thereby closing the loop between epidemiology and decision making.

Measurement error and strategic misreporting. Self-reported health data suffer from both random noise and strategic bias. Empirical research demonstrates that self-reported health behaviors such as vaccination status, mask-wearing compliance, and infection history are frequently misreported, especially when disclosure could affect employment, travel, or social standing [4, 24]. Statistical corrections (e.g. weighting, imputation) address random error but struggle with incentive-driven deception. Our work complements these efforts by modeling misreporting endogenously and quantifying how it degrades policy performance across incentive regimes.

Signaling games and equilibrium selection. Information asymmetries in public health have often been modeled as signaling or screening games where individuals send costly messages and the PHA responds with incentives or restrictions. Equilibrium refinements (separating, pooling, mixed) determine whether truth telling, deception, or mixed strategies persist. Beyond traditional one-shot or static analyses, recent work has examined, in other domains, strategic disclosure under multiple alternatives [2] and learning-induced dynamics that deviate from Nash equilibria [14]. In our work, we study the joint evolution of equilibrium strategies, epidemic dynamics, and responsive policy measures.

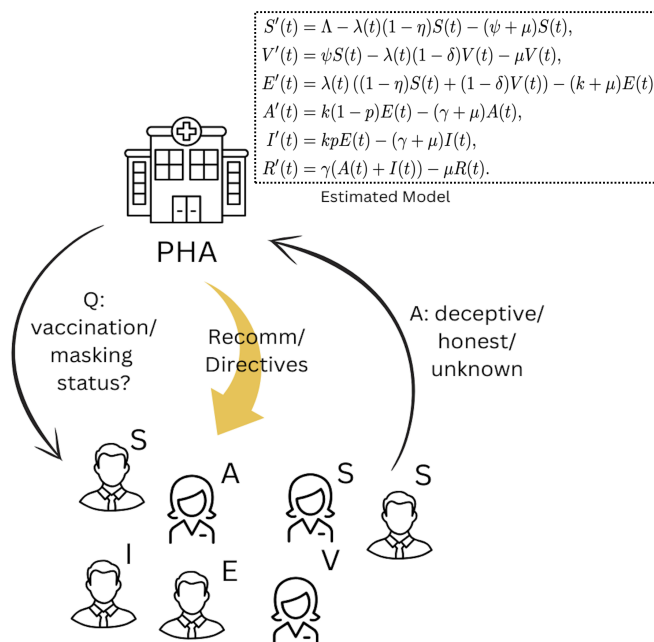


Figure 1: Illustration of the signaling game framework.

3 Framework

Basics. We model interactions between the PHA and individuals as a two-way conversation, as illustrated in Figure 1. In this model, the PHA queries individuals about their vaccination and masking status. A subset of people respond, with their answers reflecting individual behaviors (honesty or deception). Besides this information (which is not necessarily accurate), the only ground truth information available to the PHA is the number of hospitalizations (which is typically obtained by aggregating across all clinics and hospitals in its jurisdiction). It is reasonable to assume that the number of people hospitalized is equal to a fraction of the number of people infected by the virus [13]. Details of such estimation and modeling of other compartments in the SVEAIR model are covered later. Based on the response from population about their masking and vaccination, the PHA updates its epidemiological model and provides recommendations to the public on protective strategies to adopt.

Epidemiological model. We cast the interaction between the population and the PHA as a two-player signaling game \mathcal{G} , in which individual behaviors (types), reported responses (messages), and PHA strategies (actions) are drawn from discrete sets. Let t denote time. In \mathcal{G} , the sender T is a group of individuals \mathcal{K} , comprising $K(t)$ members, each in one of several epidemiological states: susceptible (S), vaccinated (V), exposed (E), symptomatic (I), asymptomatic (A), or recovered (R). Individuals send messages $m \in \mathcal{M}$ to the receiver R , with \mathcal{M} denoting the feasible set of messages. The receiver R represents the PHA’s epidemiological model, which tracks the evolution of these states through a system of ODEs [8]. The epidemiological model, essentially a variant of the SVEAIR approach, is described in Appendix A and illustrated in Figure 2. It is important to note the vaccination rate ψ and the masking rate η in this model, both of which reduce the contact rate.

Realistic assumptions for vaccination and masking. In the weekly interactive loop between individuals and the PHA (see details in Appendix D), masking compliance is defined based on self-reported frequency over the prior 5–7 days, classifying “all of the time” or “most of the time” as masking and other responses as non-masking, consistent with large-scale survey practice [34]. To account for the distinctions of vaccination and masking behaviours, the deception rates are pre-specified as 5-15% and 40-80%, respectively [19, 1].

Signaling game. For the signaling game \mathcal{G} , individuals communicate messages from a set \mathcal{M} , representing vaccination and masking status. We encode messages as two bits $b_1 b_2$, where $b_1 = 0$ (1) indicates “Vaccinated” (“Unvaccinated”), and $b_2 = 0$ (1) indicates “Masking” (“Not Masking”). Note that 0 denotes desirable behavior (i.e., desired by the PHA) on the part of individuals. Reported messages may, of course, not match actual behavior, e.g., an unvaccinated

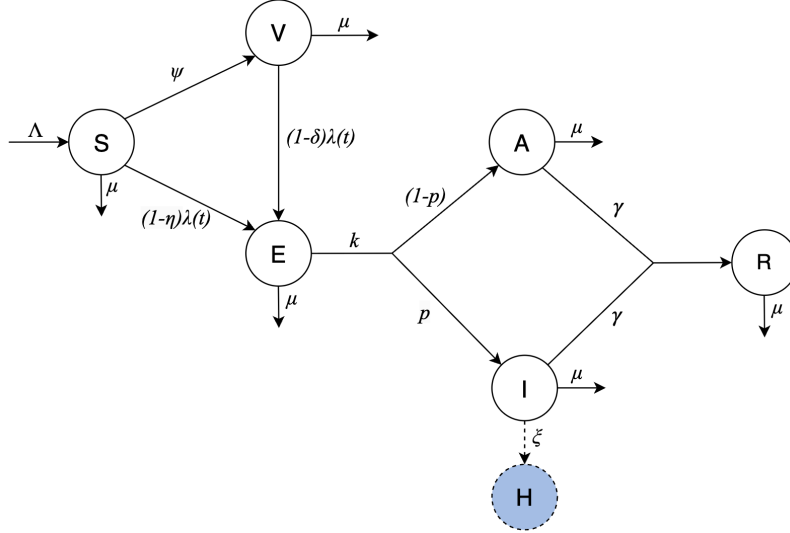


Figure 2: Compartmental SVEAIR epidemiological model with vaccination and masking. The ‘H’ is not a separate compartment but denotes (observed) hospitalization numbers, typically a fraction of the true numbers from the infected compartment.

or non-masking individual may claim otherwise, allowing the capture of deception. While we restrict attention to vaccination and masking, the framework generalizes to richer behavioral states. Further, we assume that only $M \leq K$ individuals in group \mathcal{K} report their status. Individual types are represented by $c = [c_1, \dots, c_K]^T$, where $c_i = 1$ denotes honesty and $c_i = 0$ indicates deception. Let $g(m | c)$ denote the probability of sending message m given type c . Since persistent dishonesty reduces payoffs (via penalties and social costs), deceptive individuals adopt probabilistic strategies balancing truth and misreporting. The receiver, in turn, forms beliefs about c to update the epidemiological model (Appendix A), where $\hat{\psi}$ and $\hat{\eta}$ denote estimated vaccination and contact rates, respectively. We now define sender and receiver payoffs.

Sender utility function. Falsely claiming to be vaccinated may offer incentives, such as earning more in the workplace. Similarly, falsely stating compliance with mask-wearing may help avoid penalties imposed by the PHA. In short, while honesty about individual actions may support the societal goal of achieving zero infection rates, it could negatively impact individual payoffs. Motivated by these considerations, the expected payoffs for the sender can be defined as follows:

$$U_s = \sum_k U_s^{(k)}(c_k, m_k), \quad (1)$$

where

$$\begin{aligned} U_s^{(k)}(c_k, m_k) &= g(m_k = \text{“00”} | c_k = 0)(I_v + I_m) \\ &+ g(m_k = \text{“01”} | c_k = 0)I_v \\ &+ g(m_k = \text{“10”} | c_k = 0)I_m. \end{aligned} \quad (2)$$

Here, to compute the utility, which is the incentive upon deceiving, we consider only individuals who are either not vaccinated or have not followed masking guidelines. For instance, $g(m_k = \text{“00”} | c_k = 0)$ denotes a scenario where the individual has neither adopted vaccination nor masking, yet falsely communicates that they have. In (2), I_v and I_m are the incentives for communicating falsely about vaccination and masking, respectively. Maximizing solely $U_s^{(k)}(c_k, m_k)$ leads to a trivial solution where the individuals always choose to be dishonest about their strategies, since that will bring them maximum payoffs. This leads to increased infection rates, closing down of businesses, and potentially punitive measures by the PHA. Therefore, the sender in our model is interpreted as *a representative population agent* rather than single strategic individuals. The population consists of a continuum of individuals facing identical incentives but potentially making heterogeneous reporting choices. Accordingly, the sender’s strategy $g(m | c)$ represents a population-level mixed strategy, i.e., the empirical distribution of reports generated by individuals under the same incentive structure. In this way, the sender communication strategies must represent a balance between maximizing $U_s^{(k)}(c_k, m_k)$ and minimizing these losses.

We represent the losses as proportional to the negative of semantic accuracy, which is defined as the accuracy with which the receiver interprets the individual types from the messages communicated and written as:

$$U_L(p, q) = -\frac{1}{K} \sum_{i \in \mathcal{K}} \sum_{j \in \mathcal{M}} p_{ij} q_{ji}, \quad (3)$$

where $p_{ij} = g(m_j | c_i)$ and $q_{ji} = q(c_i | m_j)$, where $q(c_i | m_j)$ is inference distribution at the receive side. For individuals that do not respond to the PHA, we set $p_{ij} = q_{ji} = 0$. The sender's objective is to find a communication policy $g(m_k | c_k)$ by maximizing the following objective:

$$\mathcal{P}_1 : [g(m_k | c_k)^*]_{\forall k} = \arg \max_{g(m_k | c_k), \forall k} (U_s - \lambda_1 U_L), \quad (4)$$

where λ_1 is a weighting factor that represents an optimal trade-off between maximizing U_s and minimizing U_L .

Next, to understand the implications of user misreporting, we define the control reproduction number R_c as the rate at which a person can pass on the infection. The expression for R_c follows directly from [8], as

$$R_c(\psi, \eta) = \underbrace{\frac{\beta k}{(k + \mu)(\gamma + \mu)}}_{R_0} \frac{(1 - \delta)\psi + (1 - \eta)\mu}{\psi + \mu}. \quad (5)$$

A value of $R_c(\psi, \eta) > 1$ represents endemic equilibrium, where the disease remains endemic in the population. Here $\beta = \beta_0(p + b(1 - p))$ indicates the weighted transmission rate considering both symptomatic and asymptomatic cases. Eqn. 5 means that as $R_c(\psi, \eta)$ increases, it may have severe consequences of the functioning of business, schools and other institutions. This will adversely impact the payoffs of each individual, in terms of loss of job or restrictions to the number of employees that can work, thereby reducing their salary or benefits. In practice, the reproduction number can be estimated using the available observations [30] by the PHA, such as hospitalization. To capture this estimation, we modify the sender payoffs as follows:

$$\begin{aligned} U_s^{(k)}(c_k, m_k) &= g(m_k = \text{"11"} | c_k) e^{-a R_c(\psi, \eta)} (I_v + I_m) \\ &+ g(m_k = \text{"10"} | c_k) e^{-a R_c(\psi, \eta)} I_v \\ &+ g(m_k = \text{"01"} | c_k) e^{-a R_c(\psi, \eta)} I_m, \end{aligned} \quad (6)$$

where a is the economic factor, which is a constant coefficient that controls the slope of the exponential curve.

As per (6), higher $R_c(\psi, \eta)$ lowers individual payoffs. Stricter PHA measures thus reflect both rising infection rates and their economic impact on daily life. The modified sender payoffs ensure that $U_s^{(k)}$ depends not only on individual strategies but also on the PHA's ability to predict and control the epidemic without disrupting normal activities.

Receiver utility function. The receiver's objective here is to model accurately the epidemiological ODEs in (22) using the estimated values of $\hat{\psi}$, $\hat{\eta}$, $\hat{\lambda}$, and $\hat{\gamma}$. We define $\theta(t) = \{\hat{\psi}(t), \hat{\eta}(t), \hat{\lambda}(t), \hat{\gamma}(t)\}$. The estimated ODE by the PHA has the same structure as the original (ground truth one) and given in Appendix A. The estimation error will typically be given by $|X(t) - \hat{X}(t)|^2$ for $X \in S, V, E, I, A, R$. However, the PHA cannot compute this error directly due to lack of access to ground-truth ODEs (as noted earlier). Fortunately, it can estimate hospitalizations—assumed to be a fixed fraction of infections [13]—and write the estimated hospitalization count as: $H(t) = \xi I(t)$, where ξ is a constant between 0 and 1. The receiver's objective is to minimize this error and thereby ensure that the protection strategies followed by it are enough to control the disease. For a given sender type and policy, the average value of the error (also called distortion) can be written as (this error should only be in terms of hospitalizations):

$$D(t) = \sum_{\mathbf{c}} p(\mathbf{c} | \mathbf{m}(t)) \sum_{\theta(t)} p(\theta(t) | \mathbf{c}) |H(t) - \hat{H}(t)|^2. \quad (7)$$

This distortion measure is used to add a fudge factor to the recommendation strategies which are computed based on PHA's perception of ODEs. The PHA's recommendation of ψ and η , defined as ψ_r and η_r , respectively, will be based on the estimated vaccination and social distancing rate as well as the evolution of error (7). Hence, we write:

$$\begin{aligned} \psi_r(t) &= \hat{\psi}(t) + \tilde{\psi}(t) \\ \eta_r(t) &= \hat{\eta}(t) + \tilde{\eta}(t). \end{aligned} \quad (8)$$

Here, the receiver aims to minimize the surprise on receiving a certain information about the epidemiological state through signaling game, while ensuring that the distortion is below a threshold. Hence, the receiver objective can be written as:

$$\begin{aligned} \mathcal{P}_2 : \arg \min_{p(\mathbf{c} | \mathbf{m})} & -\ln(p(\mathbf{c} | \mathbf{m})) \\ \text{s.t. } & D \leq D^*, \end{aligned} \quad (9)$$

where $-\ln(p(\mathbf{c} | \mathbf{m}))$ is defined as the surprise, inspired from other domains (e.g., [36]).

Using the utilities defined above, we further formulate the solutions of the signaling game defined using the tuple $(\mathcal{K}, \mathcal{C}, \mathcal{M}, \mathcal{M}_t, \mathcal{M}_r)$, where \mathcal{C} is the set of user behavior types. The Nash equilibrium (NE) strategies \mathcal{M}_t (sender) and \mathcal{M}_r (receiver) are such that for all \mathbf{c} , $\forall p(c_k | m_k) \in \mathcal{M}_r$, and $\forall g(m_k | c_k) \in \mathcal{M}_t$, we obtain

$$\begin{aligned} [g(m_k | c_k)]_{\forall k}^* &= \arg \max_{g(m_k | c_k), \forall k} (U_s - \lambda_1 U_L), \\ [p(\mathbf{c} | \mathbf{m})] &= \arg \max_{p(\mathbf{c} | \mathbf{m}), \theta} \ln(p(\mathbf{c} | \mathbf{m})) - \lambda_2 D. \end{aligned} \quad (10)$$

Game solution. A pragmatic receiver would try to compute the posterior distribution as follows:

$$P_L(\mathbf{c} | \mathbf{m}) \propto P_S(\mathbf{m} | \mathbf{c})P(\mathbf{c}). \quad (11)$$

Here, considering parallels to Shannon's rate distortion theory [9], a pragmatic transmitter would compute a transmission strategy, so as to maximize its utility for a fixed PHA recommendations:

$$P_S(\mathbf{m} | \mathbf{c}) \propto e^{\alpha(\sum_k U_s^k(c_k, m_k) - \lambda U_L(c_k, m_k))}. \quad (12)$$

Further, given the transmitter (population) policy, receiver aims to minimize the surprise on receiving the messages from the population while ensuring that the distortion remains below a threshold. At the receiver, we consider that $P(\mathbf{m})$ is known. Further, we can write the augmented Lagrangian for the receiver objective as follows:

$$\begin{aligned} & - \sum_{\mathbf{c}, \mathbf{m}} P(\mathbf{c} | \mathbf{m})P(\mathbf{m}) \ln P(\mathbf{c} | \mathbf{m}) \\ & - \lambda \sum_{\mathbf{c}, \mathbf{m}} P(\mathbf{m})p(\mathbf{c} | \mathbf{m}) \sum_{\theta} p(\theta | \mathbf{c}) \left| H - \widehat{H} \right|^2. \end{aligned} \quad (13)$$

The average surprise $-\sum_{\mathbf{c}, \mathbf{m}} P(\mathbf{c} | \mathbf{m})P(\mathbf{m}) \ln P(\mathbf{c} | \mathbf{m})$ is a convex function of $P(\mathbf{c} | \mathbf{m})$, given $\ln(x)$ is a concave function of x . Hence, the augmented Lagrangian in (13) is a convex function. Hence, to find out a minimizer, we take the derivative with respect to $P(\mathbf{c} | \mathbf{m})$. Hence, we obtain a closed form expression for the inference distribution as:

$$P(\mathbf{m}) \log P(\mathbf{c} | \mathbf{m}) + P(\mathbf{m}) - \lambda \sum_{\theta} P(\mathbf{m})p(\theta | \mathbf{c}) \left| H - \widehat{H} \right|^2 \quad (14)$$

Solving for $P(\mathbf{c} | \mathbf{m})$ leads to the following expression.

$$P(\mathbf{c} | \mathbf{m}) \propto e^{\frac{\lambda_2 \sum_{\theta} P(\mathbf{m})p(\theta | \mathbf{c}) | H - \widehat{H} |^2 - P(\mathbf{m})}{P(\mathbf{m})}} \quad (15)$$

We compute θ , which involves the vaccination and masking strategies by the PHA using (3). From the control reproduction number $R_c(\psi, \eta)$, we can write a threshold vaccination rate as follows:

$$\psi_{HI} = \frac{\mu(R_0(1 - \eta) - 1)}{1 - R_0(1 - \delta)}, \quad (16)$$

where $1 < R_0 < \frac{1}{1 - \delta}$.

4 Equilibrium Analysis

Pooling equilibrium. A pooling equilibrium [17] is achieved when all the non-compliant individuals are dishonest. In this case, the messages communicated do not convey any information about the true behavioral strategies of the population, and the PHA must rely solely on prior information and aggregate observations, such as the hospitalization signal $H(t)$.

Theorem 1. *Suppose all non-compliant individuals strictly prefer misreporting over truthful reporting for both vaccination and masking, i.e.,*

$$U_s^{lie} > U_s^{truth}$$

for all non-compliant types. Then there exists a pooling equilibrium in which all individuals report full compliance, i.e., $m_k = 00$ for all $k \in \mathcal{K}_c$, and the receiver's posterior beliefs coincide with the prior distribution over types.

Separating equilibrium. A separating equilibrium [5] is achieved when all non-compliant individuals are honest. In this case, the reported messages perfectly reveal individuals' true behaviors, enabling the PHA to accurately infer risk and select interventions such that the controlled reproduction number falls below one, with the induced policy intensity $\hat{\psi}$ exceeding the herd-immunity threshold ψ_{HI} .

Theorem 2. *If all responsive individuals report truthfully, i.e., $m_k = c_k$ for all $k \in \mathcal{K}_c$, then the signaling game admits a separating equilibrium. In this equilibrium, the PHA recovers unbiased estimates of behavioral parameters (ψ, η) and can select policies such that*

$$R_c(\psi, \eta) < 1 \quad \text{and} \quad \hat{\psi} > \psi_{HI},$$

ensuring convergence to a disease-free equilibrium.

Partial pooling equilibrium. Departing from the extreme pooling equilibrium and the idealized separating equilibrium, a partial pooling equilibrium arises when some individuals report truthfully while others engage in deception. This is captured by the mixing factor α . In this case, although self-reported signals are imperfect, the PHA may still extract partial information and attempt to enforce policies satisfying $R_c(\psi, \eta) < 1$ and $\hat{\psi} > \psi_{HI}$.

Theorem 3. *Consider the signaling game \mathcal{G} with sender utility weight λ_1 on semantic accuracy, masking incentive I_m , economic factor a , and population type distribution $(\pi_{00}, \pi_{01}, \pi_{10}, \pi_{11})$. Define the controlled reproduction numbers $R_c(0)$ under full separation and $R_c(1)$ under full pooling, with sensitivity $\beta = \frac{dR_c}{d\alpha} \Big|_{\alpha=0} > 0$.*

1. **Existence.** *A partial pooling equilibrium with mixing probability $\alpha^* \in (0, 1)$ exists if and only if the semantic weight satisfies:*

$$e^{-aR_c(1)} I_m < \lambda_1 < e^{-aR_c(0)} I_m + a\beta e^{-aR_c(0)} I_m. \quad (17)$$

2. **Characterization.** *When the existence condition holds, the equilibrium mixing probability α^* satisfies the fixed-point equation:*

$$\alpha^* = \frac{e^{-aR_c(\alpha^*)} I_m}{\lambda_1 (1 - p(\theta_{01} | m = 00))}, \quad (18)$$

where $p(\theta_{01} | m = 00) = \frac{\alpha^* \pi_{01}}{\pi_{00} + \alpha^* (\pi_{01} + \pi_{10}) + \pi_{11}}$ is the posterior belief that a pooling message originated from type θ_{01} .

3. **Approximation.** *For small deviations from separation (small α), the equilibrium mixing probability admits the closed-form approximation:*

$$\alpha^* \approx \frac{e^{-aR_c(0)} I_m}{\lambda_1 + a\beta e^{-aR_c(0)} I_m}. \quad (19)$$

Proof. See Appendix C.2. □

The bound in (17) reveals that partial pooling emerges only when the semantic accuracy weight λ_1 lies in an intermediate range: for small λ_1 incentives dominate and all non-compliant individuals pool ($\alpha = 1$); for large λ_1 accuracy dominates and all individuals separate ($\alpha = 0$).

We decompose the population \mathcal{K} into \mathcal{K}_c , the set of individuals responding to PHA queries, and \mathcal{K}_s , the set of silent individuals. The aggregate deception level \tilde{m} is defined as:

$$\begin{aligned} \tilde{m} &= \frac{1}{2} \sum_{k \in \mathcal{K}_c} \sum_{m_k} g(m_k | c_k) \|m_k - m_k^{(*)}\|_H + \frac{1}{2} \sum_{k \in \mathcal{K}_s} 2 \\ &= \frac{1}{2} \sum_{k \in \mathcal{K}_c} \sum_{m_k} g(m_k | c_k) \|m_k - m_k^{(*)}\|_H + |\mathcal{K}_s|, \end{aligned} \quad (20)$$

where $\|m_k - m_k^{(*)}\|_H$ denotes the Hamming distance between the reported message and the ground-truth behavior.

Using gradient descent, the PHA updates the policy correction term $\tilde{\psi}$ as:

$$\tilde{\psi}_t = \tilde{\psi}_{t-1} + \alpha \nabla_{\tilde{\psi}} D(t), \quad (21)$$

with the objective of ensuring $\psi^* + \tilde{\psi} > \psi_{HI}$.

5 Experimental Results

Experimental settings. We simulate $n = 50$ Monte Carlo runs of a $K=10,000$ -person SVEAIR population over 26 weeks following the two stage loop of individuals reporting and PHA modeling as shown in Figure 1. Experiments span a factorial grid of equilibrium types, policy adaptivity, and experimental settings, evaluated on epidemiological, behavioral, and strategic metrics. Details about simulation rules and evaluation procedures are provided in Appendix E.

Interactive feedback between population and PHA drives effective epidemic control. To reflect the real-world settings, we consider two regimes: (1) low baseline behavioral rates ($\psi = 0.005$, $\eta = 0.01$), representing adverse conditions in which protective behaviors are largely neglected, and (2) high baseline behavioral rates ($\psi = 0.05$, $\eta = 0.10$), corresponding to more favorable conditions. Figure 3 shows the evolution of R_c across equilibria compared against a no-interaction baseline. Under low baseline rates (Figure 3a), the separating and partial pooling equilibria achieve epidemic control ($R_c < 1$) at week 11 and 22. Pooling fails to reach the epidemic threshold within the simulation horizon, indicating sustained transmission due to severely degraded information quality. When initial behaviors are better (Figure 3b), all three equilibria achieve control with different speeds: separating (week 6), partial pooling (week 8), pooling (week 13). In both scenarios, the no-interaction baseline remains $R_c > 1$, demonstrating that adaptive, behavior-informed feedback between the population and the PHA is essential for maintaining effective epidemic control.

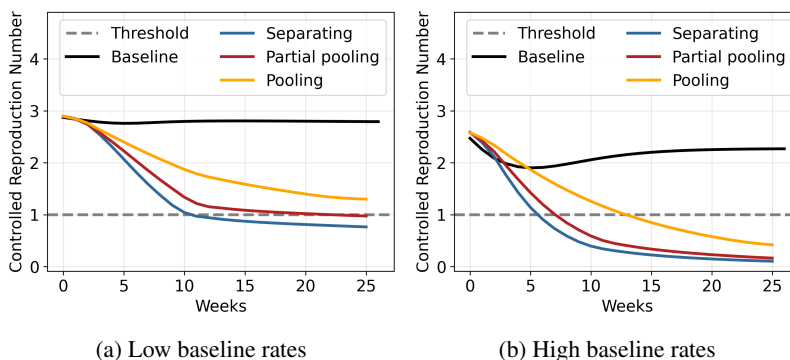


Figure 3: Controlled reproduction number (R_c) across equilibria vs no-interaction baseline with different initial behavioral rates.

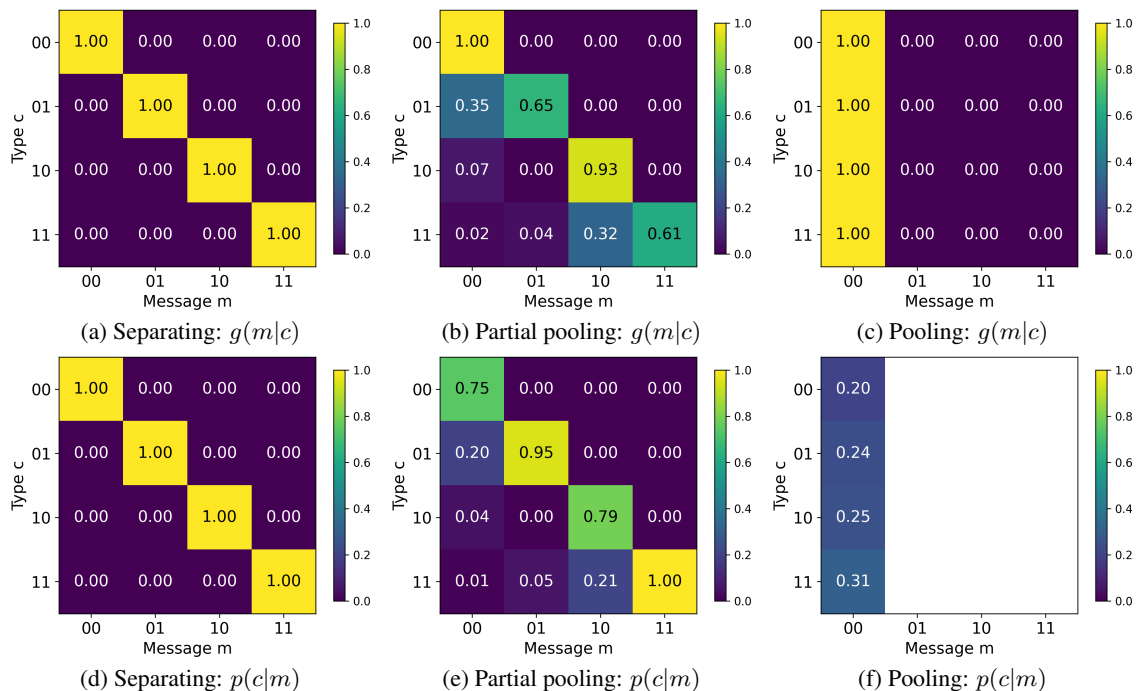


Figure 4: Sender strategies and receiver beliefs across equilibria.

Even imperfect signals carry actionable information for the PHA about population behavior. Figure 4 shows sender’s strategy $g(m|c)$ and receiver’s belief $p(c|m)$ by end of period. In separating, each type reports truthfully thus receiver’s posterior perfectly recovers true types (Figure 4a, 4d). In pooling, all types send the same message, so the receiver’s belief collapses to the prior (Figure 4c, 4f). In partial pooling, while dishonest reporting by non-compliant types introduces ambiguity, informative posteriors are still recovered (Figure 4b, 4e).

Adaptive, signal-informed policy supports epidemic mitigation. To quantify the value of behavioral information, we benchmark our adaptive, signal-informed PHA response against a random policy that ignores the information of reports under partial pooling with low initial behavioral rates. Under the adaptive policy, R_c falls below one at week 22, associated with lower peak hospitalization (0.0037 vs 0.0058) (Figure 5a, 5f); whereas under the random policy disease not controlled. Adaptive feedback drives vaccination and masking intensity near their caps between weeks 3–10 (Figure 5b, 5g), producing rapid gains in coverage to roughly 60% by week 10, compared to below 20% under random control (Figure 5c, 5h); despite higher early deception, the overall deception rate plateaus at 0.4 vs a stable ~ 0.5 under random policy (Figure 5d), and more rapid growth of information content bits grow much faster, indicating more informative signals received by the PHA (Figure 5i). Sender utility rises more under adaptive control (from 0.24 to 0.34) than under random (0.31), and receiver utility is markedly higher, peaking near 6 versus staying below 1.5 (Figure 5e, 5j). Similar patterns across equilibria and initial compliance are shown in Appendix F.1, where the overall quality of control follows the expected ordering separating $>$ partial pooling $>$ pooling.

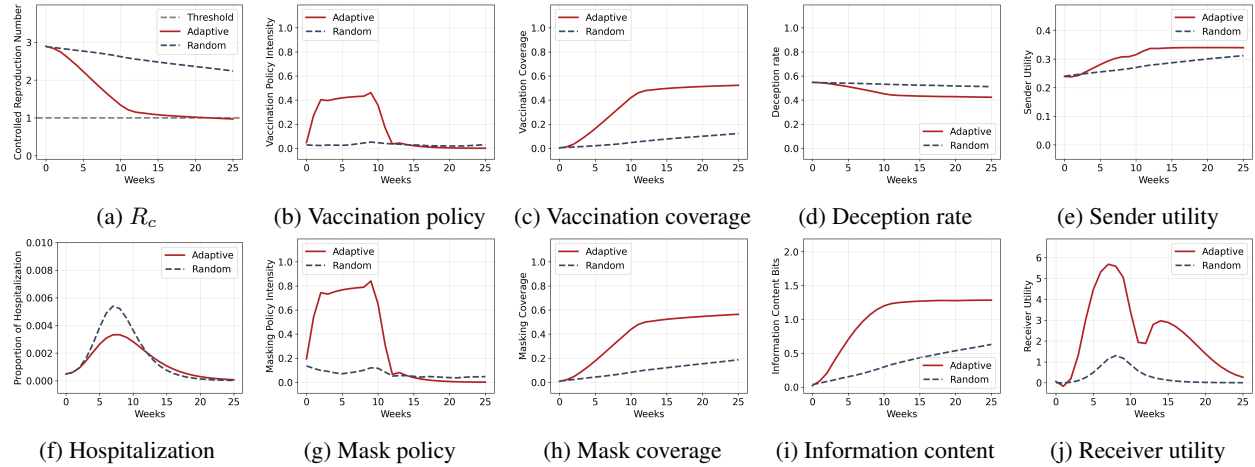


Figure 5: Comparison of adaptive and random policies under partial pooling with low initial behavioral rates, across epidemic dynamics, policy actions, signaling behavior, and utilities.

Signaling game equilibria govern persistent deception patterns. The overall deception rate and separate deception rates for vaccination and masking are shown in Figure 6. Under low baseline rates (Figure 6a), pooling exhibits the highest deception: the overall deception rate starts near 1.0 and declines toward about 0.7 by week 26. Partial pooling has intermediate deception, decreasing from 0.55 to 0.42, while separating maintains the lowest and most stable deception at 0.30 (reflection of non-responsive share). Within each equilibrium, masking deception (dotted curves) is consistently higher than vaccination deception (dashed curves), indicating that individuals are more easily misreport masking. The same ordering persists when baseline rates are high (Figure 6b). Partial pooling shows a pronounced decline in masking deception, falling from above 0.5 to near 0.35 by week 26. Separating remains 0.3. These results highlight that equilibrium structure dominates the level of dishonesty (pooling being the most deceptive), and that higher initial behavioral rates modestly reduces deceptive reporting.

Robustness of the SVEAIR–signaling-game pipeline to stress factors across equilibria. To validate our simulation framework, we perform a series of stress tests on key factors, including infection–hospitalization ratios (IHRs), incentives for vaccination and masking, the non-responsive share (NRS) to surveys, and vaccine efficacy. Table 1 and Figure A1 summarize how robust epidemic control is to these perturbations under all equilibria. Differences in disease control scores and ratios of peak hospitalization are reported relative to the baseline setting defined in Table A2. As expected, across all equilibria, doubling IHR doubles peak hospitalization, with disease control improving only under pooling. Increases in vaccine efficacy lead to lower peak hospitalization and improved the disease control score most noticeably under partial pooling. By contrast, increasing incentives or NRS has much smaller effects because they mainly perturb how honestly people report.

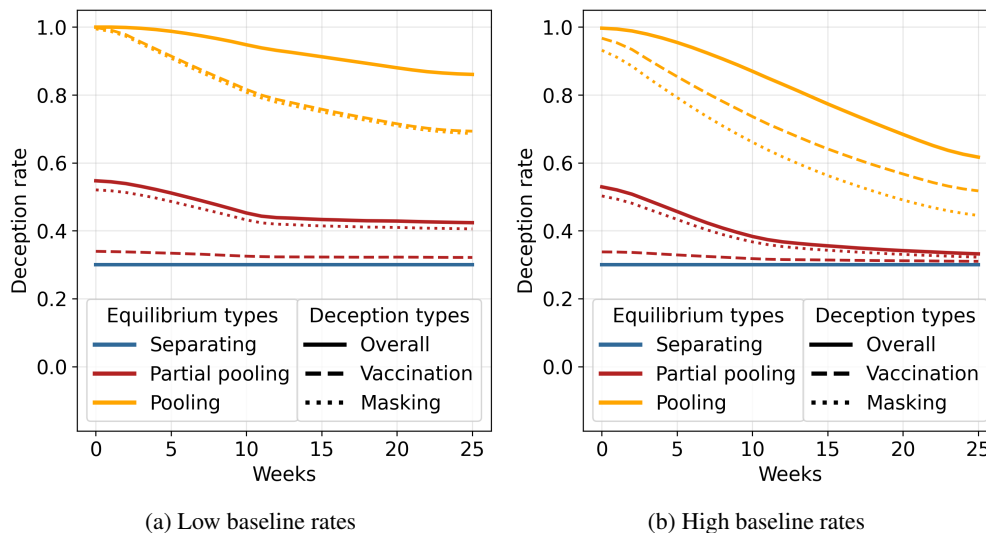


Figure 6: The deception rates across equilibria with different initial behavioral rates.

Table 1: Stress-test outcomes for different factors across equilibria. Disease control score entries show improvements (+) or degradations (-) relative to the baseline, and peak hospitalization entries show multiplicative changes relative to the baseline peak.

Factor	Disease Control Score (Δ vs Baseline)			Peak Hospitalization (Ratio vs Baseline)		
	Separating	Partial pooling	Pooling	Separating	Partial pooling	Pooling
Infection-hospitalization ratio	0.000	0.000	0.115	2.000	2.002	2.005
Incentives	0.000	-0.077	0.000	0.998	1.003	1.002
Non-responsive share	0.000	-0.038	0.000	1.002	1.004	1.002
Vaccine Efficacy	0.077	0.423	0.000	0.551	0.572	0.616

6 Limitations

Our framework makes several simplifying assumptions that can be relaxed in future work. First, the SVEAIR dynamics and the signaling layer are calibrated at the population level and do not capture heterogeneity, which may reshape epidemic trajectories and signals. Second, we fix the non-responsive share and treat non-response as maximally deceptive. Real-world non-response may be partially explained by logistical rather than strategic evasiveness. Finally, we consider a single PHA with a fixed adaptive rule. Richer policy classes (e.g., multi-agent PHAs) could change the relative performance of equilibria and policies.

7 Conclusion

This paper integrates a dynamic SVEAIR epidemic model with a game-theoretic signaling framework to study how strategic misreporting of vaccination and masking affects epidemic control and policy response. Our results reveal main insights. Equilibrium structure largely determines both the informational content of self-reported behaviors and the achievable quality of control: separating $>$ partial pooling $>$ pooling. Even with nontrivial deception, infections can still be brought under control governed by signal-informed policy.

In future work, we plan to extend our framework to state-dependent deception, and richer message spaces. Such extensions would allow us to study how misreporting itself spreads over contact networks, and how PHAs can design feedback rules that remain effective in the face of decentralized, adaptive behavioral responses.

References

- [1] Patrick M Archambault et al. “Accuracy of Self-Reported COVID-19 Vaccination Status Compared With a Public Health Vaccination Registry in Québec: Observational Diagnostic Study”. In: *JMIR Public Health Surveill* 9 (June 2023), e44465. URL: <http://www.ncbi.nlm.nih.gov/pubmed/37327046>.
- [2] Amos Azaria et al. “Strategic Information Disclosure to People with Multiple Alternatives”. In: *ACM Trans. Intell. Syst. Technol.* 5.4 (Dec. 2015). ISSN: 2157-6904. DOI: 10.1145/2558397. URL: <https://doi.org/10.1145/2558397>.
- [3] Sandipan Banerjee and Yongsheng Lian. “Data driven covid-19 spread prediction based on mobility and mask mandate information”. In: *Applied Intelligence* 52.2 (2022), pp. 1969–1978. ISSN: 0924-669X. DOI: 10.1007/s10489-021-02381-8.
- [4] M. P. Battaglia, T. M. Ezzati-Rice, and E. R. Zell. *Respondent Characteristics associated with Misreporting of Vaccinations in a Telephone Survey*. Tech. rep. CDC Methodology of the National Immunization Survey, 1997.
- [5] C. T. Bergstrom, S. Számádó, and M. Lachmann. “Separating equilibria in continuous signalling games”. In: *Philosophical Transactions of the Royal Society of London. Series B: Biological Sciences* 357.1427 (2002), pp. 1595–1606.
- [6] Lena Böff et al. “Dynamics of contact behaviour by self-reported COVID-19 vaccination and infection status during the COVID-19 pandemic in Germany: an analysis of two large population-based studies”. In: *BMC Medicine* 23.1 (2025), p. 406. DOI: 10.1186/s12916-025-04211-x.
- [7] Michal Canetti et al. “Six-Month Follow-up after a Fourth BNT162b2 Vaccine Dose”. In: *New England Journal of Medicine* 387.22 (2022), pp. 2092–2094. DOI: 10.1056/NEJMc2211283. eprint: <https://www.nejm.org/doi/pdf/10.1056/NEJMc2211283>. URL: <https://www.nejm.org/doi/full/10.1056/NEJMc2211283>.
- [8] W. Choi and E. Shim. “Optimal strategies for vaccination and social distancing in a game-theoretic epidemiologic model”. In: *Journal of theoretical biology* 505 (Nov. 2020).
- [9] T. M. Cover and J. A. Thomas. “Rate distortion theory”. In: *Elements of Information Theory*. 1991, pp. 336–373.
- [10] Matthew F. Daley et al. “Influenza vaccination accuracy among adults: Self-report compared with electronic health record data”. In: *Vaccine* 42.11 (2024), pp. 2740–2746. URL: <https://www.sciencedirect.com/science/article/pii/S0264410X24003396>.
- [11] Fatimah S. Dawood et al. “Interim Estimates of 2019–20 Seasonal Influenza Vaccine Effectiveness – United States, February 2020”. In: *MMWR. Morbidity and Mortality Weekly Report* 69.7 (2020). Epub 2020 Feb 21, pp. 177–182. ISSN: 1545-861X. DOI: 10.15585/mmwr.mm6907a1. URL: <https://doi.org/10.15585/mmwr.mm6907a1>.
- [12] J. Degen. “The rational speech act framework”. In: *Annual Review of Linguistics*. Vol. 9. 1. New York, NY: Springer US, 2023, pp. 519–540.
- [13] S. J. Fox et al. “Real-time pandemic surveillance using hospital admissions and mobility data”. In: *Proceedings of the National Academy of Sciences*. Vol. 119. 7. 2022.
- [14] Yuma Fujimoto, Kaito Ariu, and Kenshi Abe. “Learning in Multi-Memory Games Triggers Complex Dynamics Diverging from Nash Equilibrium”. In: *Proceedings of the Thirty-Second International Joint Conference on Artificial Intelligence, IJCAI-23*. Ed. by Edith Elkind. Main Track. International Joint Conferences on Artificial Intelligence Organization, Aug. 2023, pp. 118–125. DOI: 10.24963/ijcai.2023/14. URL: <https://doi.org/10.24963/ijcai.2023/14>.
- [15] Jeremy Howard et al. “An evidence review of face masks against COVID-19”. In: *Proceedings of the National Academy of Sciences* 118.4 (2021), e2014564118. DOI: 10.1073/pnas.2014564118. eprint: <https://www.pnas.org/doi/pdf/10.1073/pnas.2014564118>. URL: <https://www.pnas.org/doi/abs/10.1073/pnas.2014564118>.
- [16] Laura P. Hurley et al. “Accuracy of self-reported vaccination status using surveys in safety-net, integrated and rural health systems in Colorado”. In: *Vaccine* 72 (2026), p. 128101. URL: <https://www.sciencedirect.com/science/article/pii/S0264410X25013994>.
- [17] S. Huttegger, B. Skyrms and P. Tarres, and E. Wagner. “Some dynamics of signaling games”. In: *Proceedings of the National Academy of Sciences* 111.3 (2014), pp. 10873–10880.
- [18] Stephanie A. Irving et al. “Evaluation of self-reported and registry-based influenza vaccination status in a Wisconsin cohort”. In: *Vaccine* 27.47 (2009), pp. 6546–6549. URL: <https://www.sciencedirect.com/science/article/pii/S0264410X09012353>.
- [19] Aleksandra Jakubowski et al. “Self-reported vs Directly Observed Face Mask Use in Kenya”. In: *JAMA Network Open* 4.7 (July 2021), e2118830–e2118830. ISSN: 2574-3805. DOI: 10.1001/jamanetworkopen.2021.18830. eprint: https://jamanetwork.com/journals/jamanetworkopen/articlepdf/2782566/jakubowski_2021_id_210154_1627056043.52861.pdf. URL: <https://doi.org/10.1001/jamanetworkopen.2021.18830>.

- [20] Min Jing et al. “COVID-19 modelling by time-varying transmission rate associated with mobility trend of driving via Apple Maps”. In: *Journal of Biomedical Informatics* 122 (2021), p. 103905. ISSN: 1532-0464. DOI: <https://doi.org/10.1016/j.jbi.2021.103905>. URL: <https://www.sciencedirect.com/science/article/pii/S1532046421002343>.
- [21] C. Koprulu and F. Djeumou and. “Neural stochastic differential equations for uncertainty-aware offline RL”. In: *Thirteenth International Conference on Learning Representations*. Singapore, Apr. 2025.
- [22] Andrea Gurmankin Levy et al. “Misrepresentation and Nonadherence Regarding COVID-19 Public Health Measures”. In: *JAMA Network Open* 5.10 (2022), e2235837. DOI: 10.1001/jamanetworkopen.2022.35837.
- [23] Jr. Longini Ira M. et al. “Containing Pandemic Influenza with Antiviral Agents”. In: *American Journal of Epidemiology* 159.7 (Apr. 2004), pp. 623–633. ISSN: 0002-9262. DOI: 10.1093/aje/kwh092. eprint: <https://academic.oup.com/aje/article-pdf/159/7/623/160052/kwh092.pdf>. URL: <https://doi.org/10.1093/aje/kwh092>.
- [24] Wilson N. Merrell, Soyeon Choi, and Joshua M. Ackerman. “When and Why People Conceal Infectious Disease”. In: *Psychological Science* 35.3 (2024), pp. 215–225. DOI: 10.1177/09567976231221990.
- [25] S. Milanesi and G. D. Nicolao. “Correction of Italian under-reporting in the first COVID-19 wave via age-specific deconvolution of hospital admissions”. In: *arXiv*. <https://doi.org/10.48550/arxiv.2307.09978> (2023).
- [26] Melahat Melek Oguz. “Improving influenza vaccination uptake among healthcare workers by on-site influenza vaccination campaign in a tertiary children hospital”. In: *Human Vaccines & Immunotherapeutics* 15.5 (2019). Epub 2019 Mar 19, pp. 1060–1065. ISSN: 2164-554X. DOI: 10.1080/21645515.2019.1575164. URL: <https://doi.org/10.1080/21645515.2019.1575164>.
- [27] R. Patel, I. M. Longini Jr, and M. E. Halloran. “Finding optimal vaccination strategies for pandemic influenza using genetic algorithms”. In: *Journal of theoretical biology* 234.2 (2005), pp. 201–212.
- [28] G. Pullano et al. “Underdetection of cases of COVID-19 in France threatens epidemic control”. In: *Nature* 590.7844 (2021), pp. 134–139.
- [29] Timothy C. Reluga and Alison P. Galvani. “A general approach for population games with application to vaccination”. In: *Mathematical Biosciences* 230.2 (2011), pp. 67–78. ISSN: 0025-5564. DOI: <https://doi.org/10.1016/j.mbs.2011.01.003>. URL: <https://www.sciencedirect.com/science/article/pii/S0025556411000101>.
- [30] J. Shi, Y. Zhou, and J. Huang. “Unlocking the Power of Time-Since-Infection Models: Data Augmentation for Improved Instantaneous Reproduction Number Estimation”. In: *arXiv*. <https://doi.org/10.48550/arXiv.2403.12243> (2025).
- [31] Lauren J. Shiman et al. ““Be honest and gain trust”: a population health study to understand the factors associated with building trust in local government related to COVID-19 and vaccination in three historically disinvested neighborhoods in New York City”. In: *Frontiers in Public Health* 11 (2023), p. 1285152. DOI: 10.3389/fpubh.2023.1285152.
- [32] J. Sobel. “Signaling games”. In: *Complex social and behavioral systems: Game theory and agent-based models*. New York, NY: Springer US, 2020, pp. 251–268.
- [33] M. W. Tanner, L. Sattenspiel, and L. Ntaimo. “Finding optimal vaccination strategies under parameter uncertainty using stochastic programming”. In: *Mathematical biosciences* 215.2 (2008), pp. 144–151.
- [34] Juliana C Taube, Zachary Susswein, and Shweta Bansal. “Spatiotemporal Trends in Self-Reported Mask-Wearing Behavior in the United States: Analysis of a Large Cross-sectional Survey”. In: *JMIR Public Health Surveill* 9 (Mar. 2023), e42128. ISSN: 2369-2960. DOI: 10.2196/42128. URL: <http://www.ncbi.nlm.nih.gov/pubmed/36877548>.
- [35] Jayaraman J. Thiagarajan et al. “Machine Learning-Powered Mitigation Policy Optimization in Epidemiological Models”. In: *Proceedings of the 1st Workshop on Healthcare AI and COVID-19, ICML 2022*. Vol. 184. Proceedings of Machine Learning Research. PMLR, 2022, pp. 63–72. URL: <https://proceedings.mlr.press/v184/thiagarajan22a.html>.
- [36] C. K. Thomas and W. Saad. “Neuro-Symbolic Causal Reasoning Meets Signaling Game for Emergent Semantic Communications”. In: *IEEE Transactions on Wireless Communications* 23.5 (May 2024).
- [37] Kieran A. Walsh et al. “The duration of infectiousness of individuals infected with SARS-CoV-2”. In: *Journal of Infection* 81.6 (2020), pp. 847–856. ISSN: 0163-4453. DOI: 10.1016/j.jinf.2020.10.009. URL: <https://doi.org/10.1016/j.jinf.2020.10.009>.
- [38] G. Wan, Z. Liu, X. Shan, et al. “EARTH: Epidemiology-Aware Neural ODE with Continuous Disease Transmission Graph”. In: *Forty-second International Conference on Machine Learning*. 2025.
- [39] S. L. Wu et al. “Substantial underestimation of SARS-CoV-2 infection in the United States”. In: *Nature Communications* 11.1 (2020).
- [40] Youqi Yang et al. “Exploring the Big Data Paradox for various estimands using vaccination data from the global COVID-19 Trends and Impact Survey (CTIS)”. In: *Science Advances* 10.22 (2024), eadj0266. URL: <https://www.science.org/doi/abs/10.1126/sciadv.adj0266>.

A Epidemiological Model

The epidemiological model studied in this paper is given by:

$$\begin{aligned}
S'(t) &= \Lambda - \lambda(t)(1 - \eta)S(t) - (\psi + \mu)S(t), \\
V'(t) &= \psi S(t) - \lambda(t)(1 - \delta)V(t) - \mu V(t), \\
E'(t) &= \lambda(t)((1 - \eta)S(t) + (1 - \delta)V(t)) - (k + \mu)E(t), \\
A'(t) &= k(1 - p)E(t) - (\gamma + \mu)A(t), \\
I'(t) &= kpE(t) - (\gamma + \mu)I(t), \\
R'(t) &= \gamma(A(t) + I(t)) - \mu R(t),
\end{aligned} \tag{22}$$

where $X'(t) = \frac{dX(t)}{dt}$. We define the vaccination rate as ψ ($0 \leq \psi \leq 1$) and the masking rate as η ($0 \leq \eta \leq 1$), indicating that susceptible individuals reduce the contact rate by a fraction of η . Vaccine efficiency is described using the factor δ , which quantifies the rate of reduction in infection rate for vaccinated individuals. Disease-free individuals enter the susceptible class through birth or immigration at a constant rate Λ and their natural death rate is denoted by μ . It is assumed that susceptible individuals become infected at a rate of $\lambda(t) = \frac{\beta_0(t)(I(t) + bA(t))}{K(t)}$. Here, β_0 is the transmission rate, b is the rate of relative infectiousness of asymptomatic cases compared to symptomatic cases, and $K(t) = S(t) + V(t) + E(t) + I(t) + A(t) + R(t)$. We define $1/k$ as the duration of the latent period, which is defined as the time between when a person is exposed to the disease and when they become infectious. We also assume that a proportion p of infected individuals become symptomatic. Both symptomatic and asymptomatic individuals are assumed to recover at a rate of γ .

Likewise, the ODE model estimated by the receiver (i.e., the PHA) is given by:

$$\begin{aligned}
\hat{S}'(t) &= \Lambda - \hat{\lambda}(t)(1 - \hat{\eta})\hat{S}(t) - (\hat{\psi} + \mu)\hat{S}(t), \\
\hat{V}'(t) &= \hat{\psi}\hat{S}(t) - \hat{\lambda}(t)(1 - \delta)\hat{V}(t) - \mu\hat{V}(t), \\
\hat{E}'(t) &= \hat{\lambda}(t)\left((1 - \hat{\eta})\hat{S}(t) + (1 - \delta)\hat{V}(t)\right) - (k + \mu)\hat{E}(t), \\
\hat{A}'(t) &= k(1 - p)\hat{E}(t) - (\hat{\gamma} + \mu)\hat{A}(t), \\
\hat{I}'(t) &= kp\hat{E}(t) - (\hat{\gamma} + \mu)\hat{I}(t), \\
\hat{R}'(t) &= \hat{\gamma}(\hat{A}(t) + \hat{I}(t)) - \mu\hat{R}(t).
\end{aligned} \tag{23}$$

B Behavioral Types

Table A1 denote 9 behavioral types of individuals capturing their true status and how they report their vaccination and/or masking status. To interpret the ‘True Status’ column, note that 0 indicates compliance and 1 indicates non-compliance. The first number in the True Status column is meant for vaccination status and the second number denotes masking status. In row 2, for instance, the true status is 01, i.e., the individual is vaccinated but not masking. However, this individual reports 00 (i.e., they are honest about their vaccination status but deceptive about their masking status). The number of possible types is not a true cross-product because individuals who are masked or who are vaccinated are assumed to have no incentive to lie about their status. Thus there is a ‘Deceptive’ value in a row only if the corresponding entry in True Status is a 1 (i.e., non-compliance).

C Equilibrium Characterization

C.1 Pooling equilibrium

In pooling, all types send the same message $m^* = 00$ (claim full compliance). Here, the sender Strategy can be written as:

$$g^*(m|c) = \begin{cases} 1 & \text{if } m = 00 \\ 0 & \text{otherwise} \end{cases} \quad \forall c \tag{24}$$

Table A1: Nine behavioral types defined in terms of how people with different compliance combinations report truthfully or deceive about their vaccination and/or masking status. (See A.2 for explanation.)

Type	True status	Vaccine report	Mask report
T_1	00	0 (Honest)	0 (Honest)
T_2	01	0 (Honest)	0 (Deceptive)
T_3	01	0 (Honest)	1 (Honest)
T_4	10	0 (Deceptive)	0 (Honest)
T_5	10	1 (Honest)	0 (Honest)
T_6	11	0 (Deceptive)	0 (Deceptive)
T_7	11	0 (Deceptive)	1 (Honest)
T_8	11	1 (Honest)	0 (Deceptive)
T_9	11	1 (Honest)	1 (Honest)

Receiver Belief can be written as:

$$p^*(c | m = 00) = p(c) \quad (\text{prior probability}) \quad (25)$$

The PHA learns nothing from messages and must rely on prior population compliance rates and observable hospitalizations $H(t)$. Pooling exists when deviating to truth-telling is not profitable. For a non-compliant individual ($c \neq 00$): $U_s(m = 00 | c) \geq U_s(m = c | c)$. This holds when incentives dominate semantic accuracy. $I_v + I_m \succ \frac{1}{|M|} \cdot \frac{1}{K}$.

$$e^{-aR_c^{\text{pooling}}}(I_v + I_m) > \lambda_1 \cdot K^{-1}$$

Receiver's Best Response: Under pooling, the PHA must estimate $\hat{\omega}, \hat{\epsilon}$ from hospitalizations alone, i.e.,

$$\begin{aligned} \hat{\psi}(t) &= \omega_0 + \psi_\Delta(t) \\ \hat{\eta}(t) &= \eta + \eta_\Delta(t), \end{aligned}$$

Where corrections ψ_Δ, η_Δ solve:

$$\min_{\psi_\Delta, \eta_\Delta} \left| H(t) - \xi \hat{I}(t; \psi + \psi_\Delta, \eta + \eta_\Delta) \right|^2$$

subject to distortion constraint: $D(t) \leq D^*$. *Deception Rate* can be written as: $\tilde{m}^* = \frac{1}{2} \sum_{k \in K_c} \|m_k - c_k\|_H + |K_s|$, where $\|m_k - c_k\|_H$ is Hamming distance. In pure pooling with $m = 00$ for all, we obtain $\tilde{m}^* = \frac{1}{2}|K_c| \cdot \mathbb{E}[\|00 - c\|_H] + |K_s|$. If population has baseline rates (ψ^*, η^*) (round truth), then we get

$$\begin{aligned} \tilde{m}^* &= |K_c|(1 - \psi^*)(1 - \eta^*) + \frac{1}{2}|K_c|\psi^*(1 - \eta^*) \\ &\quad + \frac{1}{2}|K_c|(1 - \psi^*)\eta^* + |K_s|. \end{aligned} \quad (26)$$

C.2 Partial pooling equilibrium

Here, some users separate and others pool, with mixing probability defined as α . We consider a simplistic model of sender strategy as written below:

$$g^*(m|c) = \begin{cases} 1 & \text{if } c = 00 \text{ and } m = 00 \\ \alpha & \text{if } c \in \{01, 10\} \text{ and } m = 00 \\ 1 - \alpha & \text{if } c \in \{01, 10\} \text{ and } m = c \\ 1 & \text{if } c = 11 \text{ and } m = 00 \\ 0 & \text{otherwise} \end{cases} \quad (27)$$

Let: π_{00} represents fraction truly compliant (vaccinated + masking), π_{01} represents fraction vaccinated but not masking π_{10} represents fraction masking but not vaccinated, and π_{11} represents fraction non-compliant on both, with $\pi_{00} + \pi_{01} + \pi_{10} + \pi_{11} = 1$. Given mixing probability α , the proportion sending each message becomes,

$$\begin{aligned} P(m = 00) &= \pi_{00} + \alpha(\pi_{01} + \pi_{10}) + \pi_{11} \\ P(m = 01) &= (1 - \alpha)\pi_{01} \\ P(m = 10) &= (1 - \alpha)\pi_{10} \\ P(m = 11) &= 0 \quad (\text{no one admits full non-compliance}) \end{aligned} \quad (28)$$

Using Bayes' rule, when PHA receives $m = 00$, and θ_{ij} representing the estimate of type "ij",

$$\begin{aligned} p(\theta_{00} | m = 00) &= \frac{\pi_{00}}{\pi_{00} + \alpha(\pi_{01} + \pi_{10}) + \pi_{11}} \\ p(\theta_{01} | m = 00) &= \frac{\alpha\pi_{01}}{\pi_{00} + \alpha(\pi_{01} + \pi_{10}) + \pi_{11}} \\ p(\theta_{10} | m = 00) &= \frac{\alpha\pi_{10}}{\pi_{00} + \alpha(\pi_{01} + \pi_{10}) + \pi_{11}} \\ p(\theta_{11} | m = 00) &= \frac{\pi_{11}}{\pi_{00} + \alpha(\pi_{01} + \pi_{10}) + \pi_{11}} \end{aligned} \quad (29)$$

The PHA estimates vaccination rate as:

$$\hat{\psi}(\alpha) = \pi_{00} + \pi_{01} + \alpha\pi_{10} + \pi_{11} \quad (30)$$

$$\hat{\eta}(\alpha) = \pi_{00} + \pi_{10} + \alpha\pi_{01} + \pi_{11} \quad (31)$$

Similarly for masking:

$$\hat{\epsilon}(\alpha) = P(m = 00) \cdot \frac{\pi_{00} + \alpha\pi_{10}}{\pi_{00} + \alpha(\pi_{01} + \pi_{10}) + \pi_{11}} + (1 - \alpha)\pi_{10} \quad (32)$$

Key observation: $\hat{\psi}(\alpha)$ and $\hat{\eta}(\alpha)$ are overestimates of true compliance because of pooling. From eq. (5), $R_c(\alpha) = R_c(\hat{\psi}, \hat{\eta})$. As α increases (indicating more pooling), $\hat{\psi}(\alpha)$ and $\hat{\eta}(\alpha)$ both increase because the PHA believes more individuals are vaccinated and masking, even though true compliance remains unchanged; consequently, the PHA under-responds, leading to an increase in $R_c(\alpha)$. The semantic accuracy term can be written when the actual type is θ_{01} as:

$$U_{L,\text{pool}}^{01}(\alpha) = \alpha \cdot p(\theta_{01} | m = 00) + (1 - \alpha) \quad (33)$$

For type θ_{01} pooling:

$$U_{\text{pool}}^{01}(\alpha) = e^{-aR_c(\alpha)} I_m + \lambda_1 \cdot [\alpha \cdot p(\theta_{01} | m = 00) + (1 - \alpha)], \quad (34)$$

and for type θ_{01} separating:

$$U_{L,\text{sep}}^{01} = 0 + \lambda_1 \cdot 1 = \lambda_1 \quad (35)$$

For optimal mixing, we need $U_{\text{pool}}^{01}(\alpha^*) = U_{\text{sep}}^{01}$. This leads to:

$$e^{-aR_c(\alpha^*)} I_m + \lambda_1 [\alpha^* \cdot p(\theta_{01} | m = 00) + (1 - \alpha^*)] = \lambda_1 \quad (36)$$

Simplifying this, we obtain

$$\alpha^* = \frac{e^{-aR_c(\alpha^*)} I_m}{\lambda_1 [1 - p(\theta_{01} | m = 00)]}. \quad (37)$$

Substituting Bayes' rule, we obtain:

$$e^{-aR_c(\alpha^*)} I_m = \lambda_1 \alpha^* \left[1 - \frac{\alpha^* \pi_{01}}{\pi_{00} + \alpha^* (\pi_{01} + \pi_{10}) + \pi_{11}} \right] \quad (38)$$

This is an implicit equation in α^* because $R_c(\alpha^*)$ depends on α^* and the right-hand side contains α^* in a nonlinear way. Therefore, it generally requires a numerical solution. For small deviations from separation, we use a linear approximation:

$$R_c(\alpha) \approx R_c(0) + \beta\alpha \quad (39)$$

where

$$\beta = \left. \frac{dR_c}{d\alpha} \right|_{\alpha=0} > 0 \quad (40)$$

Similarly, the conditional probability can be approximated as:

$$p(\theta_{01} | m = 00) \approx \frac{\alpha\pi_{01}}{\pi_{00} + \pi_{11}} \quad (41)$$

Then, using the linear approximation for $R_c(\alpha)$ and ignoring higher-order terms, we have:

$$e^{-a[R_c(0) + \beta\alpha]} I_m \approx \lambda_1 \alpha \left[1 - \frac{\alpha\pi_{01}}{\pi_{00} + \pi_{11}} \right] \quad (42)$$

For small α , ignoring α^2 terms, this simplifies to:

$$e^{-aR_c(0)}(1 - a\beta\alpha)I_m \approx \lambda_1\alpha \quad (43)$$

Rearranging terms gives:

$$e^{-aR_c(0)}I_m \approx \lambda_1\alpha + a\beta e^{-aR_c(0)}I_m \cdot \alpha \quad (44)$$

Finally, solving for α^* yields:

$$\alpha^* \approx \frac{e^{-aR_c(0)}I_m}{\lambda_1 + a\beta e^{-aR_c(0)}I_m} \quad (45)$$

C.2.1 Existence conditions

For partial pooling equilibrium to exist, we require $0 < \alpha^* < 1$. To find a lower bound, consider when pure separation ($\alpha = 0$) is not an equilibrium. At $\alpha = 0$, suppose type θ_{01} deviates to pool. The utility from deviating is:

$$\begin{aligned} U_{L,\text{pool}}^{01}(\alpha = 0) &= e^{-aR_c(0)}I_m + \lambda_1[(1 - 0) + 0 \cdot 0] \\ &= e^{-aR_c(0)}I_m + \lambda_1. \end{aligned} \quad (46)$$

The utility from separating is:

$$U_{L,\text{sep}}(\alpha = 0) = \lambda_1 \quad (47)$$

For separation to be unstable, we need:

$$e^{-aR_c(0)}I_m + \lambda_1 > \lambda_1 \quad (48)$$

This simplifies to:

$$e^{-aR_c(0)}I_m > 0 \quad (49)$$

which is always true, implying that pure separation cannot be an equilibrium when $I_m > 0$. To determine when pure pooling ($\alpha = 1$) is not an equilibrium, note that at $\alpha = 1$, everyone pools. The conditional probability is:

$$p(\theta_{01} | m = 00) = \frac{\pi_{01}}{\pi_{00} + \pi_{01} + \pi_{10} + \pi_{11}} = \pi_{01} \quad (50)$$

The utility from pooling is:

$$\begin{aligned} U_{L,\text{pool}}(1) &= e^{-aR_c(1)}I_m + \lambda_1[(1 - 1) + 1 \cdot \pi_{01}] \\ &= e^{-aR_c(1)}I_m + \lambda_1\pi_{01} \end{aligned} \quad (51)$$

The utility from deviating to separate is:

$$U_{L,\text{sep}} = \lambda_1 \quad (52)$$

For pooling to be unstable (deviation profitable), we require:

$$e^{-aR_c(1)}I_m + \lambda_1\pi_{01} < \lambda_1 \quad (53)$$

Since $(1 - \pi_{01}) \leq 1$, the condition for pooling to be unstable simplifies to:

$$e^{-aR_c(1)}I_m < \lambda_1 \quad (54)$$

From the approximation

$$\alpha^* \approx \frac{e^{-aR_c(0)}I_m}{\lambda_1 + a\beta e^{-aR_c(0)}I_m}, \quad (55)$$

for $\alpha^* < 1$, we require:

$$e^{-aR_c(0)}I_m < \lambda_1 + a\beta e^{-aR_c(0)}I_m. \quad (56)$$

Rearranging gives:

$$e^{-aR_c(0)}I_m(1 - a\beta) < \lambda_1. \quad (57)$$

For small $a\beta$, this implies:

$$\lambda_1 > e^{-aR_c(0)}I_m - a\beta e^{-aR_c(0)}I_m. \quad (58)$$

Combining this lower bound on λ_1 with the upper bound from pooling instability, we obtain:

$$e^{-aR_c(1)}I_m < \lambda_1 < e^{-aR_c(0)}I_m + a\beta e^{-aR_c(0)}I_m. \quad (59)$$

From (59) we infer the following conclusions. The semantic weight λ_1 must lie in a Goldilocks zone for mixed to exist. If λ_1 is too low (below the lower bound), semantic accuracy does not matter much, incentives dominate, and everyone pools ($\alpha = 1$), resulting in a full pooling equilibrium. If λ_1 is too high (above the upper bound), semantic accuracy matters a lot, people value being understood correctly, and everyone separates ($\alpha = 0$), leading to a separating equilibrium. If λ_1 is just right (within the window), there is a trade-off between incentives and accuracy, and mixed occurs with $0 < \alpha^* < 1$. In this case, some individuals lie while others tell the truth, creating a stable mixing equilibrium.

C.3 Tolerance frontiers

In partial pooling equilibrium, the key question is: *to what extent can deception be tolerated while still ensuring the epidemic converges to an equilibrium with negligible infections?*

Theorem 4 (Partial Pooling and Tolerable Deception). *There exists a partial pooling equilibrium in which some non-compliant individuals misreport while others report truthfully if and only if the induced deception level \tilde{m} remains below a critical tolerance threshold \tilde{m}_{\max} such that the PHA can select policies satisfying*

$$R_c(\psi, \eta) < 1 \quad \text{and} \quad \hat{\psi} > \psi_{HI}.$$

In this regime, epidemic control is preserved despite strategic misreporting.

The population strategy that maximizes deception while preserving epidemic control can be expressed as:

$$g^*(\mathbf{m} \mid \mathbf{c}) = \arg \max_{g(\mathbf{m} \mid \mathbf{c}), \tilde{\psi}} \tilde{m} \quad \text{s.t.} \quad \psi^* + \tilde{\psi} > \psi_{HI}. \quad (60)$$

The resulting equilibrium deception level is given by:

$$\tilde{m}^* = \frac{1}{2} \sum_{k \in \mathcal{K}_c} \sum_{m_k} g^*(m_k \mid c_k) \|m_k - m_k^{(*)}\|_H + |\mathcal{K}_s|. \quad (61)$$

This characterization defines a *tolerance frontier* that quantifies how much strategic misreporting can be absorbed before epidemic control breaks down.

We further decompose the deception into vaccination and masking components. Let $h_v(m_k, m_k^{(*)}) \in \{0, 1\}$ and $h_\eta(m_k, m_k^{(*)}) \in \{0, 1\}$ denote the Hamming distance restricted to the vaccination bit and the masking bit, respectively. Then the vaccination deception $\tilde{m}^{(v)}$ and masking deception $\tilde{m}^{(\eta)}$ can be written as

$$\tilde{m}^{(v)} = \sum_{k \in \mathcal{K}_c} \sum_{m_k} g(m_k \mid c_k) h_v(m_k, m_k^{(*)}) + |\mathcal{K}_s|, \quad (62)$$

$$\tilde{m}^{(\eta)} = \sum_{k \in \mathcal{K}_c} \sum_{m_k} g(m_k \mid c_k) h_\eta(m_k, m_k^{(*)}) + |\mathcal{K}_s|. \quad (63)$$

D Weekly Interactive Loop Between Population and PHA

Algorithm 1 summarizes the iterative feedback mechanism that governs the interaction between the population and the PHA in each simulation cycle. Each week, individuals report (truthfully or deceptively) their behavioral status, and the PHA updates its epidemiological model and policy recommendations based on these reports and observed hospitalization outcomes. The two-stage loop between players sketched in Figure 1:

1. **Individuals reporting.** Individuals decide whether to reveal or to misreport their current vaccination and masking status, weighing economic incentives against the costs of deception. To reflect realistic behavioral constraints, only non-compliers who forego either vaccination or masking are eligible to lie for the corresponding behavior. Moreover, individuals in the recovered (R) compartment are barred from deception because their acquired immunity leaves them little incentive to falsify their status.
2. **Public Health Authority (PHA) updates.** The PHA receives the (possibly distorted) reports, updates its belief over population behavior, and issues revised policy recommendations for vaccination uptake and contact-rate reduction.

E Experimental Settings

As described in the main text, for each scenario considered, we run Monte-Carlo simulations of a K=10,000–person population over a 26-week horizon with the baseline parameter set listed in Table A2.

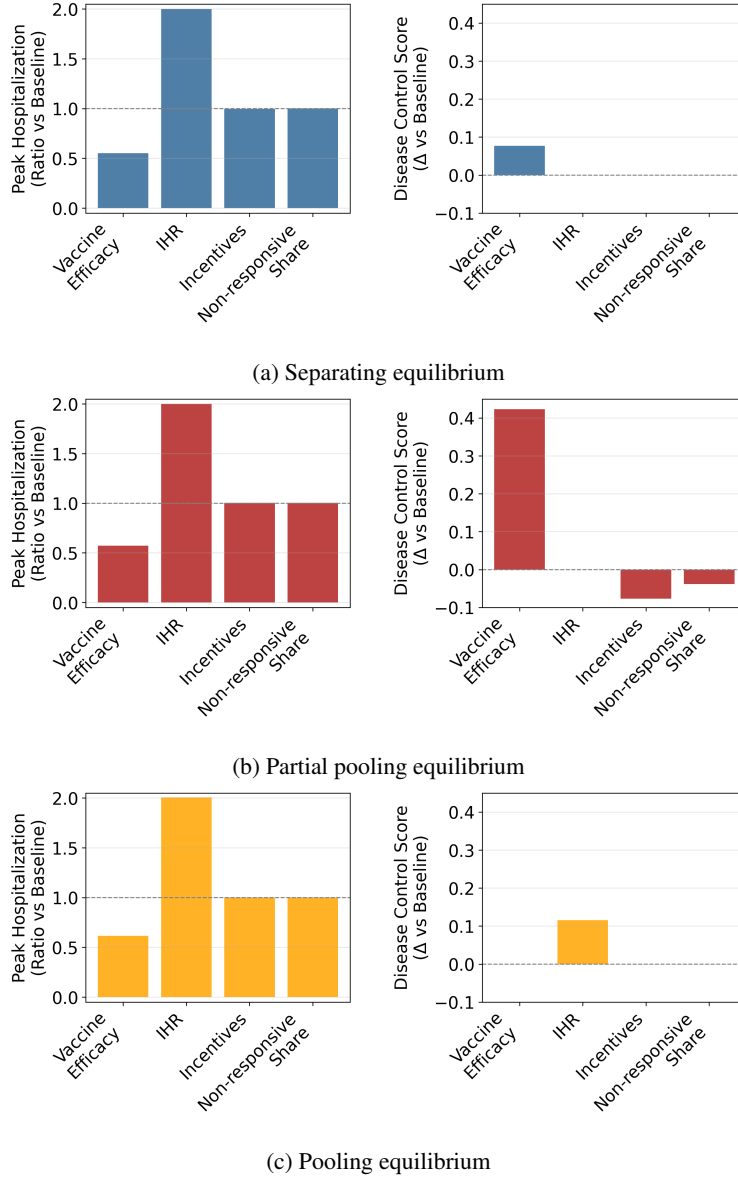


Figure A1: Sensitivity of epidemic outcomes to stress factors across equilibria.

E.1 Experimental conditions.

We evaluate the model over a full factorial grid: three equilibrium structures (separating, partial pooling, pooling) crossed with public-health policy (adaptive vs. random), baseline behavioral-rate level (low vs. high), and incentives for vaccination and masking. Daily outputs are aggregated into weekly steps. Epidemiological and behavioral series are smoothed with a Savitzky–Golay filter, whereas strategic variables are updated by exponential smoothing to retain short-term fluctuations.

E.2 Baselines.

Two baselines benchmark the two-player signaling game schemes studied here:

1. **No interaction.** Individuals never report behaviors and the PHA issues no recommendations, providing a lower-bound for epidemic control across equilibria.

Algorithm 1 Weekly Interactive Loop Between Population and PHA

Require: Initial states (S, V, E, A, I, R) , initial policies (ψ_0, η_0) , parameters $(\beta_0, k, p, \gamma, \mu, \xi)$

- 1: **for** each week $t = 1$ to T **do**
- 2: **Population reporting:**
- 3: **for** each individual $i \in \mathcal{K}$ **do**
- 4: Decide true behaviors (v_i, m_i) (vaccination, masking)
- 5: Generate reported message (\hat{v}_i, \hat{m}_i) according to equilibrium type (truthful or deceptive)
- 6: **end for**
- 7: Aggregate reports to obtain $\hat{\psi}_t, \hat{\eta}_t$, and deception rate d_t
- 8: **PHA update:**
- 9: Observe hospitalization $H_t = \xi I_t$
- 10: Use internal SVEAIR model and current beliefs to compute \hat{H}_t
- 11: Compute distortion $D_t = (H_t - \hat{H}_t)^2$
- 12: **if** $D_t > D^*$ **then**
- 13: Update policy recommendations via a gradient step:
 $\psi_{r,t} = \psi_t + \Delta_\psi, \quad \eta_{r,t} = \eta_t + \Delta_\eta$
- 14: where $(\Delta_\psi, \Delta_\eta)$ are obtained by minimizing D_t
- 15: **else**
- 16: Keep previous recommendations $(\psi_{r,t}, \eta_{r,t}) \leftarrow (\psi_t, \eta_t)$
- 17: **end if**
- 18: **Epidemic propagation:**
- 19: Integrate SVEAIR ODEs for one week using $(\psi_{r,t}, \eta_{r,t})$
- 20: Update population states $(S, V, E, A, I, R)_{t+1}$
- 21: Store weekly metrics: $R_c(t)$, deception rate d_t , distortion D_t , utilities
- 22: **end for**

2. **Random policy.** PHA replaces its adaptive rule with weekly recommendations perturbed by zero-mean noise whose variance matches the empirical variance of the adaptive policy’s gradient (estimated from hospitalisations), isolating the value of behavior-aware adaptation.

E.3 Evaluation metrics.

We measure the $week_{control}$ when R_c first falls < 1 (converted to a disease-control score as $1 - week_{control}/26$), deception rate, vaccination and masking coverage, peak hospitalization, sender utility (benefit from recommendations) and receiver distortion (cost from deviating signals).

E.4 Data and code.

All code for running simulations, generating figures, and reproducing results is available at: <https://anonymous.4open.science/r/epi-signaling-games>.

F Supplemental experimental results

F.1 Comparison of adaptive and random policies across equilibria.

Across all three information regimes, the adaptive policy consistently outperforms the random policy in epidemic control, driving lower R_c , smaller peak hospitalization, and better receiver utility. Moreover, the overall quality of control follows the expected ordering separating $>$ partial pooling $>$ pooling, with both peak hospitalization and equilibrium deception rates smallest under separating, larger under partial pooling, and largest under pooling.

An interesting nuance is that when initial compliance is already high, sender utility under the random policy is often comparable to, or slightly higher than, under adaptive control—because in that regime the epidemic can be kept in check even with relatively mild, noisy recommendations, so the population “pays” less in terms of strong, targeted interventions while still enjoying reasonably low infection risk.

Table A2: Summary of model parameters and baseline values used in our experiments.

Parameter	Description	Value	References
<i>Epidemiological model parameters</i>			
μ	Natural death rate	$1/(75 \times 365)$	[23]
β_0	Baseline transmission rate	0.35	[20]
δ	Vaccine efficacy	0.45	[11]
$1/\gamma$	Infectious period (days)	10	[37]
b	Infectiousness of asymptomatic	0.5	[23]
$1/k$	Latent period (days)	5	[29]
p	Probability exposed to infected	0.67	[23]
ξ	Hospitalization ratio	0.05	[13]
<i>Signaling-game parameters</i>			
I_v	Lying incentive for vaccination	1.0	NA
I_m	Lying incentive for masking	0.5	NA
λ_1	Weight on semantic loss	0.2	NA
α	Surprise weight in receiver utility	1.0	NA
a	Economic factor	0.5	NA
<i>Initial conditions</i>			
ψ_{init}	Baseline vaccination rate	0.05	[26]
η_{init}	Baseline masking rate	0.10	[15]
I_0	Initial infected count	150	NA
$P(K_s)$	Non-responsive population share	0.3	[40]
<i>Simulation parameters</i>			
K	Population size	10 000	NA
T	Simulation duration (weeks)	26	[7]

F.2 Stress test

Figure A1: Sensitivity of epidemic outcomes to stress factors across equilibria

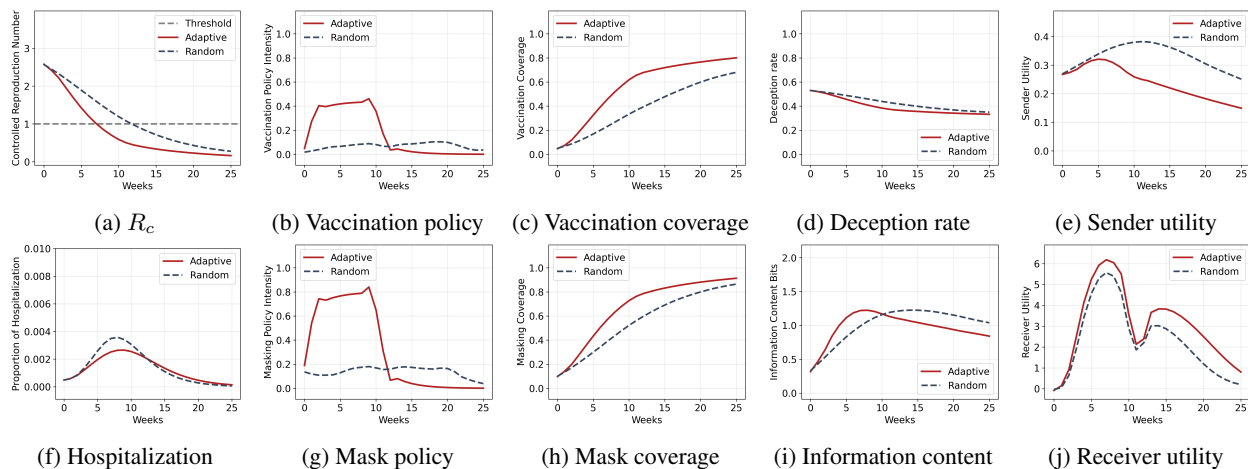


Figure A2: Comparison of adaptive and random policies under partial pooling with high initial behavioral rates, across epidemic dynamics, policy actions, signaling behavior, and utilities.

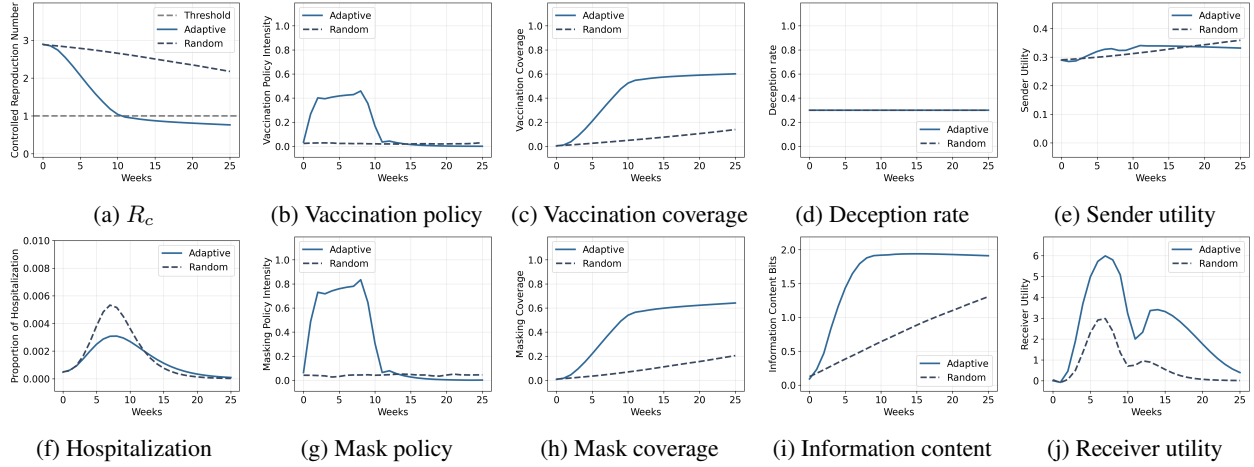


Figure A3: Comparison of two PHA policies under separating with low initial behavioral rates, across epidemic dynamics, policy actions, signaling behavior, and utilities.

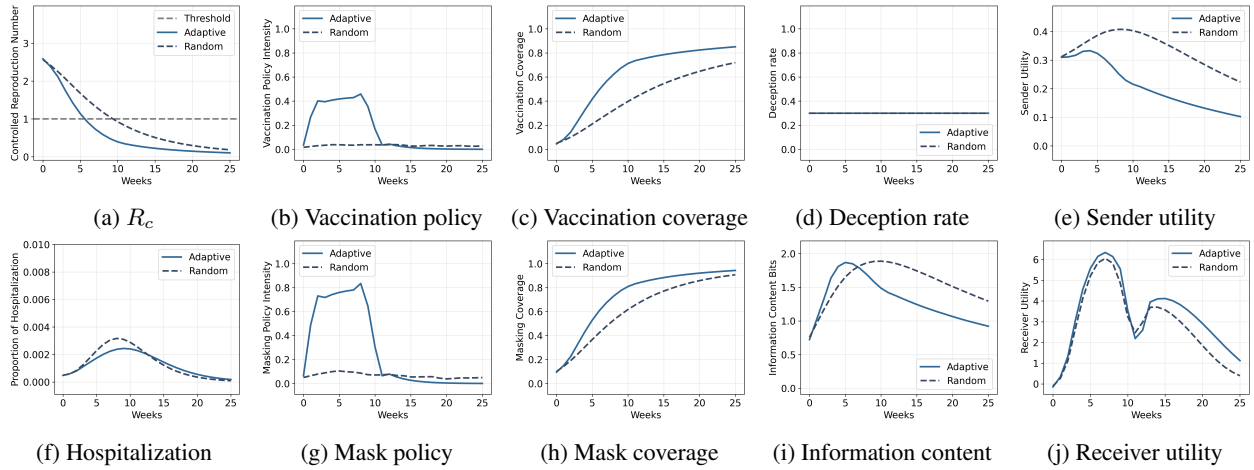


Figure A4: Comparison of two PHA policies under separating with high initial behavioral rates, across epidemic dynamics, policy actions, signaling behavior, and utilities.

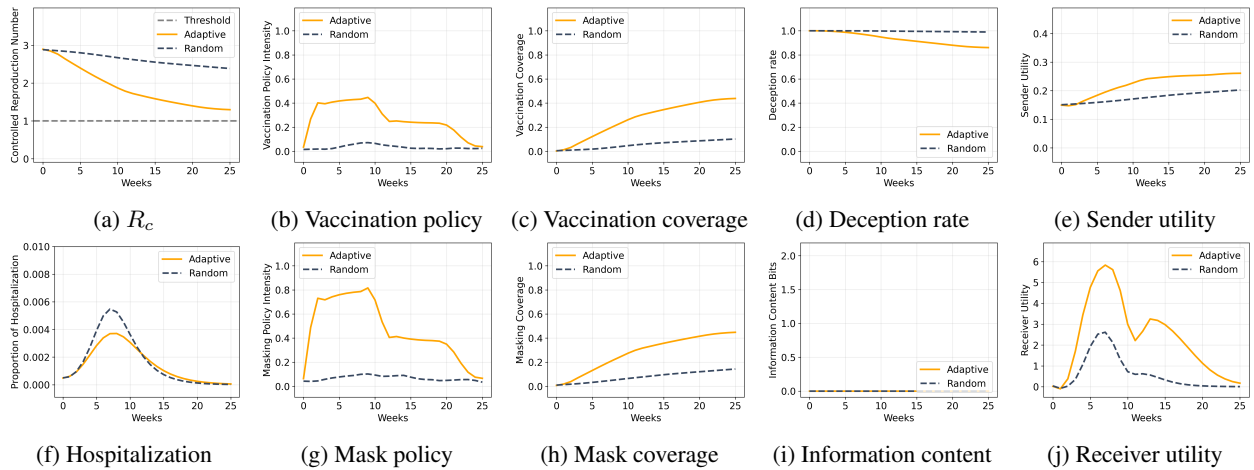


Figure A5: Comparison of two PHA policies under pooling with low initial behavioral rates, across epidemic dynamics, policy actions, signaling behavior, and utilities.

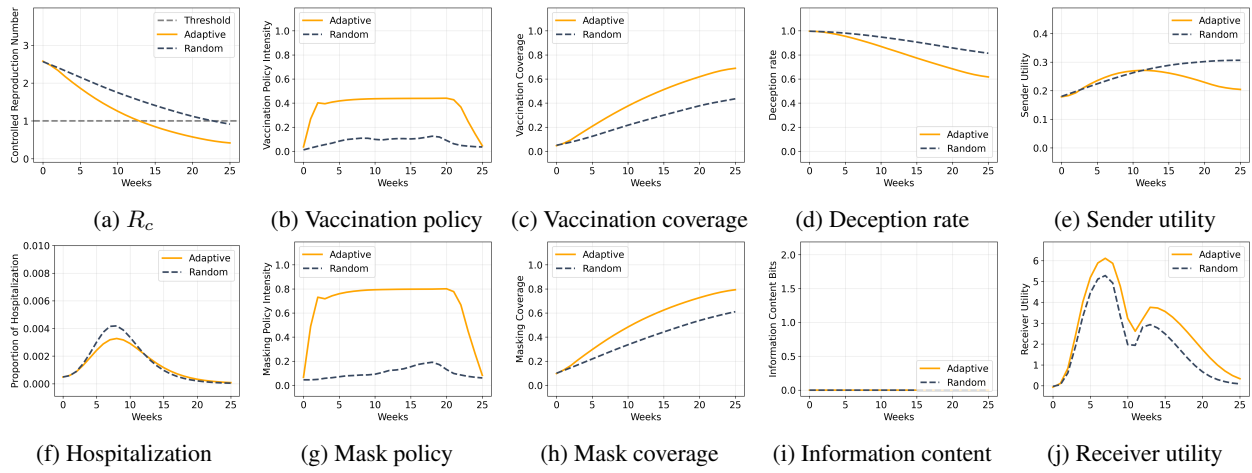


Figure A6: Comparison of two PHA policies under pooling with high initial behavioral rates, across epidemic dynamics, policy actions, signaling behavior, and utilities.